A NUMERICAL PROCEDURE FOR SIMULATION OF A HOUSEHOLD VAPOR COMPRESSION REFRIGERATION SYSTEM UNDER STEADY-STATE CONDITIONS USING HFC-134A AND HC-600A AS REFRIGERANTS

Gustavo Matana Aguiar, gustavo.matana.aguiar@usp.br
Gherhardt Ribatski, ribatski@sc.usp.br
Heat Transfer Research Group, Escola de Engenharia de São Carlos (EESC), University of São Paulo (USP), Av. Trabalhador São-Carlense, 400, São Carlos-SP, 13.566-590, Brazil

Abstract. *This work concerns the development of a mathematical model and a procedure for its numerical solution to evaluate the system-level thermal performance of a household vapor compression refrigeration cycle operating with the fluids HC-600a and HFC-134a under steady-state conditions. The hermetic compressor was modelled based on a semi-empirical approach to evaluate volumetric and overall efficiencies. To ensure numerical robustness, an explicit algebraic model was adopted for the capillary tube. The roll-bond evaporator and a wire-and-tube condenser performance were evaluated by a quasi-1D tube-fin flow model coupled with suitable pressure drop gradient and heat transfer coefficient correlations. At the end, all components were integrated and solved by an iterative procedure.*

Keywords*: vapor compression system design, adiabatic capillary tube, roll bond evaporator, wire-and-tube condenser, hermetic compressor.*

1. NOMENCLATURE

Roman Letters

A	Fitting Cte. (Eq. 2)	[m³/kg]
B	Fitting Cte. (Eq. 2)	[m³.Pa/kg]
C	Clearance volume ratio	[-]
C	Fitting Cte.	[-]
D	Diameter	[m]
D	Fitting Cte.	[-]
dz	Infinitesimal length	[m]
F	Friction factor	[-]
G	Mass flux	[kg/m².s]
H	Heat transfer coefficient	[W/m².°C]
H	Height	[m]
i	Enthalpy	[J/kg]
k	Polytropic index, Thermal conductivity	[-] [W/m.°C]
L	Length	[m]
ṁ	Mass flow rate	[kg/s]
P	Pitch	[m]
p	Pressure	[Pa]
$\dot{Q}$	Heat exchanged rate	[W]
T	Temperature	[°C]
U	Average fluid velocity	[m/s]
W	Width	[m]

Greek letters

α	Combined eff. Cte.	[-]
β	Combined eff. Cte.	[1/Pa]
ε	Emissivity	[-]
η	Efficiency	[-]
μ	Viscosity	[kg/m.s]
υ	Specific Volume	[m³/kg]
ρ	Density	[kg/m³]

Subscripts

comb	Combined
c	Compressor
cond	Condenser
d	Discharge
i	Discrete element index
evap	Evaporator
fin	Fin
f	Flashing condition
in	Inlet
out	Out
sonic	Sonic condition
s	Suction
sup	Superheating
swept	Swept
t	Tube
v	Volumetric
w	Wire

2. INTRODUCTION

According to an estimative presented in 2004 by CEPEL (Centro de Pesquisas de Energia Elétrica), the refrigerators are responsible for 28% of energy consumption in the domestic sector and 6% of total energy consumption in Brazil. So, given that the Carnot efficiency of domestic refrigerators barely reaches 15 % (Hermes & Melo, 2008), it can be speculated that there are plenty of opportunities in these equipment for further reductions on their energy consumption. The majority of techniques addressed to evaluate and optimize the refrigerator performance rely mainly on data from standardized experiments; however, numerical models can be employed likewise. The main advantages of the latter method over the former is the reduced test time and costs as well as the possibility of virtually testing an infinite set of operational conditions.

Motivated by Montreal (1989) and Kyoto (2005) Protocols, the HVAC industry is currently experiencing a shift towards the use of refrigerants with zero ODP and reduced GWP such as the HFOs and HCs. In this context, numerical models are successful employed to assess and compare the performance of the environment-friendly refrigerants with CFCs and HCFCs (Domanski & McLinden, 1992; Gossard et Al., 2013). The numerical models available in literature can be segregated as steady-state and transient models. The steady state approach is commonly used to assess whole system performance for a given operational condition in optimization analyses of performance and costs. The transient models are commonly employed to evaluate energy consumption (Hermes & Melo, 2009), evaporator frosting (Borges, Melo & Hermes, 2015) and design of control system (Kouri, Machado & Ismail, 2001). The focus of the present study is to develop a steady-state model capable of assessing the thermal and hydraulic performances of a vapor compression system of small capacity operating with refrigerants HC-600a and HFC-134a.

3. MATHEMATICAL MODEL

The refrigeration system evaluated in the present study is comprised of a hermetic compressor, wire-and-tube condenser, adiabatic capillary tube and a roll-bond evaporator. The assessment of overall system performance is based on the development and integration of sub-models for each of the four components.

3.1 Adiabatic Capillary Tube

Despite of its construction simplicity, the two-phase flow behavior inside capillary tubes is quite complex because it involves compressible flow, phase change, turbulence and metastable regions. In the present study, the mathematical submodel of the capillary tube is based on the explicit semi-empiric solution for adiabatic flows proposed by Hermes, Melo and Knabben (2010) for the refrigerants HFC-134a and HC-600a. In this work, the authors adopted the following assumptions: (i) the tube is straight, horizontal, adiabatic and presents constant cross-section geometry, (ii) the viscous compressible flow is one dimensional in the axial direction, (iii) the pressure drop at entrance and exit sections are neglected, (iv) the pressure drop due to flow acceleration is neglected because its value is an order magnitude lower than the frictional pressure drop, (v) the two-phase flow is homogeneous, (vi) the liquid specific volume is constant, (vii) the expansion of the fluid is an isenthalpic process and (viii) metastable flow does not occur.

Applying all the simplifying assumptions to the conservation of momentum, the following equation is obtained:

$$dz = \frac{2 \cdot D}{f \cdot G^2 \cdot v} dP \tag{1}$$

Based on the abovementioned assumptions, Hermes, Melo and Knabben (2010) performed an integration of Eq. (1) by splitting the tube domain in two parts: a single-phase region and a two-phase region downstream the flashing point. They approximate the two-phase specific volume according to the relationship first proposed by Yilmaz and Unal (1996) and later improved by Zhang and Ding (2004) given as follows:

$$v_f = a + \frac{b}{P_f} \tag{2}$$

where $a = v_f(1-r)$, $b = v_f P_f r$ and $r = 1.63 \cdot 10^5 P_f^{-0.72}$. In this model, the friction factor is estimated as a function of the Reynolds number of the whole mixture flowing at liquid phase of the flash point, so that $f = c \cdot Re_f^{-d}$. Based on a curve fitting of a broad experimental database, Hermes, Melo and Knabben (2010) estimated the coefficients *c* and *d* equal to 0.14 and 0.15. After the integration of Eq. (1), they obtained an explicit equation for calculating refrigerant mass flow rate as function of the inlet and outlet pressures and tube geometry given as follows:

$$\dot{m} = \left\{ \frac{\pi^{2-d} 2^{2d-3}}{c} \frac{D^{5-d}}{\mu_f^d L} \left[\frac{P_{in} - P_f}{v_f} + \frac{P_f - P_{out}}{a} + \frac{b}{a^2} \ln\left(\frac{aP_{out} + b}{aP_f + b} \right) \right] \right\}^{\frac{1}{2-d}} \tag{3}$$

where the minimum value of the exit pressure is limited by the sonic pressure, calculated as suggested by Yilmaz and Unal (1996), $P_{sonic} = G\sqrt{v_f P_f r}$. Therefore, in the present study $P_{out} = P_{evap}$ if $P_{out} > P_{sonic}$ and $P_{out} = P_{sonic}$ if $P_{out} < P_{sonic}$.

3.2 Heat Exchangers: Roll-bond Evaporator and Wire-and-tube Condenser

Both heat exchangers are modelled according to a 1-D distributed-parameters model adopting the following assumptions: (i) Steady-state operation; (ii) The tube-fin geometry is the same along the longitudinal direction of the tube, (iii) Gravitational and accelerational pressure drop parcels are neglected, (iv) the cross-sectional refrigerant properties are uniform (v) the thermal resistance of tube wall is neglected. The frictional pressure drop for single-phase flow is estimated according to the explicit relationship proposed by Coolebrok-White as suggested by Swamee and Jain (1976). For two-phase flows, the friction factor is calculated according to the correlation of Gronnerud (1979) for the two-phase multiplier, as suggested by Didi, Kattan and Thome (2002). The local pressure of each discrete volume is given as follows, assuming a constant pressure gradient along each element:

$$P_{i+1} = P_i - f_i \frac{\Delta z}{D_{int}} \frac{\rho_i {U_i}^2}{2} \tag{4}$$

The enthalpy at the exit of each discrete element is estimated as follows:

$$i_{i+1} = i_i + \frac{\dot{Q}_i}{\dot{m}} \tag{5}$$

The heat transferred throughout an infinitesimal element is computed by employing a global heat transfer coefficient analysis considering internal forced convection (single-phase flow, flow boiling and in tube condensation) and an external thermal resistance composed of convection and radiation heat transfer.

3.2.1 Evaporator

Figures 1 and 2 present schematics of the geometry of the roll-bond evaporator modeled in the present study. The fin length is defined as follows:

$$L_{fin} = \left(\frac{H_{evap} \cdot W_{evap}}{L_{evap}} - D_{evap} \right) \cdot \frac{1}{2} \tag{6}$$

where L_{evap} is given as the product of the number of passes and H_{evap}. Adiabatic tip fin is assumed.

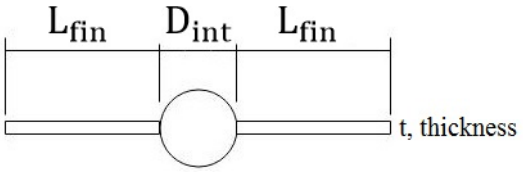

Figure 1 – Cross section view of a discrete element of the evaporator

The external heat transfer coefficient due to natural convection is calculated through the correlation of Churchill and Chu (1975) for isothermal vertical plate. The heat transfer coefficient due to radiation HTC is estimated by assuming a grey body with an emissivity ε=0.92. For both, the temperature of the isothermal plate is assumed as 2 ºC above the saturation temperature of the refrigerant at the evaporator entry condition. This hypothesis agrees with the trend of experimental data from Melo, Silva and Silveira (1998). Moreover, variations of the temperature of the isothermal plate up to 5°C affects only marginally the external heat transfer resistance. The internal heat transfer coefficient is given by the correlations of Gnielinski (1979) for single-phase flow and Liu-Winterton (1991) for convective boiling.

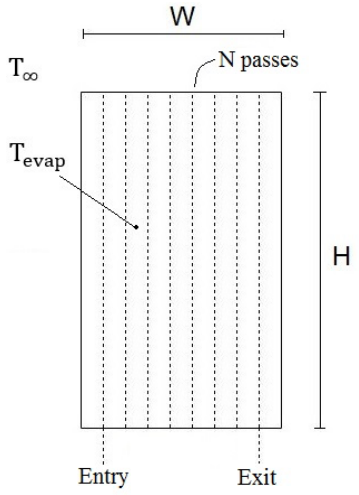

Figure 2 – Roll-bond evaporator idealized geometry

3.2.2 Condenser

The condenser is modelled as suggested by Bansal and Chin (2003). The wire-and-tube geometry and discretization scheme is shown in Fig. 3. The tube and wire pitches (p_t and p_w) are assumed as constant along the heat exchanger. Each discrete element is composed of a pair of wires soldered perpendicular to the tube with a fixed length of $\Delta z = p_w$. U-bends are not taken into account. The number of pair of wires N_w and the total refrigerant circuit length L_{cond} are calculated as follows:

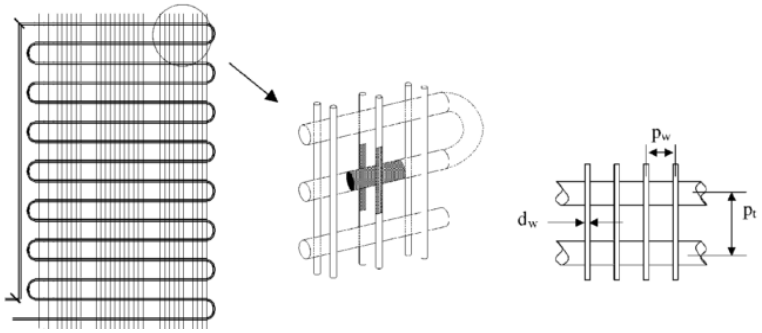

Figure 3 – Wire-and-Tube condenser geometry (Bansal and Chin, 2003)

$$N_w = \frac{W_{cond}}{p_w} \text{-} 1 \tag{6}$$

$$L_{cond} = \frac{W_{cond}}{p_w}\left(\frac{H_{cond}}{p_t} - 1\right) \tag{7}$$

where W_{cond} is the condenser width and H_{cond} is the height.

For each discrete element, the pair of wires is idealized as fins whose efficiencies are given as follows:

$$\eta_{fin_i} = \frac{tanh\left(\sqrt{\frac{4 \cdot h_{ext_i}}{k_{steel} \cdot D_w}} \cdot \frac{p_t}{2}\right)}{\sqrt{\frac{4 \cdot h_{ext_i}}{k_{steel} \cdot D_w}} \cdot \frac{p_t}{2}} \tag{8}$$

An average wire temperature is estimated based on the definition of fin efficiency:

$$T_{wire_i} = \eta_{fin_i} \cdot \left(T_{tube_i} - T_\infty\right) + T_\infty \tag{9}$$

The mean wall temperature of each discrete element is obtained by weighting the tube and wire temperatures according to their relative superficial areas as follows:

$$\overline{T}_{\Delta z_i} = \frac{(\pi D_{ext}\, p_w) T_{tube_i} + (2\pi D_{wire}\, p_t) T_{wire_i}}{(\pi D_{ext}\, p_w) + (2\pi D_{wire}\, p_t)} \tag{10}$$

The heat transferred through radiation is estimated based on the average temperature of the discrete element $\overline{T}_{\Delta z_i}$ and assuming a grey body with an emissivity ε=0.92. The external heat transfer coefficient through the natural convection mechanism is estimated as proposed by Tagliafico and Tanda (1997). The internal heat transfer coefficient for single-phase flow is calculated according to the correlation of Gnielinski (1979). The correlation of Shah (1979) is used to estimate the heat transfer coefficient for in tube condensation. An iterative procedure is necessary in order to calculate the tube temperature of each discrete element.

3.3 Hermetic Compressor

The compressor sub-model is based on the semi-empirical method developed by Jähnig, Reindl and Klein (2000). In this model, the volumetric and overall efficiencies are used to calculate the compression power and the refrigerant mass flow rate for a given operating condition. In this sub-model, the following simplification hypothesis are adopted: (i) Steady-state condition; (ii) the specific volume at the inlet and outlet of the compressor are constant; (iii) the compression/expansion processes are polytropic; and (iv) heat exchange between the compressor and the ambient is incorporated at the polytropic coefficient. The volumetric efficiency, defined as the ratio of the volumetric flow rate and the volume swept by the compressor piston is estimated according to the following equation:

$$\eta_v = 1 - C \cdot \left[\left(\frac{P_d}{P_s}\right)^{\frac{1}{k}} - 1\right] \tag{11}$$

where C is the clearance volume ratio, and k is the polytropic expansion coefficient, evaluated as the adiabatic expansion coefficient at the compressor entrance. Then, the actual mass flow rate is calculated as follows:

$$\dot{m} = \frac{\dot{V}_{swept}}{v_s} \cdot \eta_v \tag{12}$$

The compressor discharge pressure is assumed as equal to the condenser entry pressure and the pressure at suction line is approximated as the pressure at the evaporator exit multiplied by a fixed dimensionless pressure loss coefficient ($P_s = (1 - \delta P) P_{exit,evap}$). The parameters C and δP are calculated by nonlinear regression of experimental data given by the manufacturer obtained based on standard test condition such as ASHRAE 32.

The ideal compression work is calculated as the integral $\oint v dP$ over the p-v diagram of a reciprocating compressor with clearance volume and operating under polytropic processes ($Pv^k = ct.$). The actual power required by the compressor is estimated by considering the ideal compression work and a combined efficiency η_{comb}, which includes the electric motor efficiency as well as other inefficiencies such as frictional effects, as follows:

$$\eta_{comb} \cdot \dot{W}_{c_{real}} = \dot{m} \cdot P_s v_s \frac{k}{k-1} \left[\left(\frac{P_d}{P_s}\right)^{\frac{k-1}{k}} - 1\right] \tag{13}$$

The combined efficiency is assumed as a function of the evaporator pressure only and is approximated by an expression suggested by Klein and Reindl (1999) in ASHRAE RP-870 technical report, as follows:

$$\eta_{comb} = \alpha + \frac{\beta}{P_{evap}} \tag{14}$$

where the constants α and β are obtained by non-linear regression of experimental data.

4. NUMERICAL SCHEME

The system performance was assessed by a numerical routine implemented in EES platform (Klein, 2011). The four components of the system were assumed as interconnected in series, i.e. the exit thermodynamic state of refrigerant of a component is the entry state of the next component. The main objective of this procedure was to determine the P-h diagram of the vapor-compression refrigeration cycle operating under user-specified ambient and refrigerated-compartment temperatures.

An iterative procedure was used to achieve numerical convergence. Initial values of evaporator saturation temperature T_{evap}, condenser saturation temperature T_{cond} and superheating degree at evaporator exit ΔT_{sup} were assumed. The first convergence criteria is based on the conservation of mass for a steady-state system and it states that the mass flow rate of refrigerant flowing thought the capillary tube needs to be equal to the mass flow rate through the compressor within a 1% tolerance of error. The second convergence criteria consist of ensuring that the refrigerant returns to the same thermodynamic state after a full loop throughout all system components, i.e. the superheating at evaporator exit needs to be equal to the compressor entry superheating. Figure 4 summarizes the procedure.

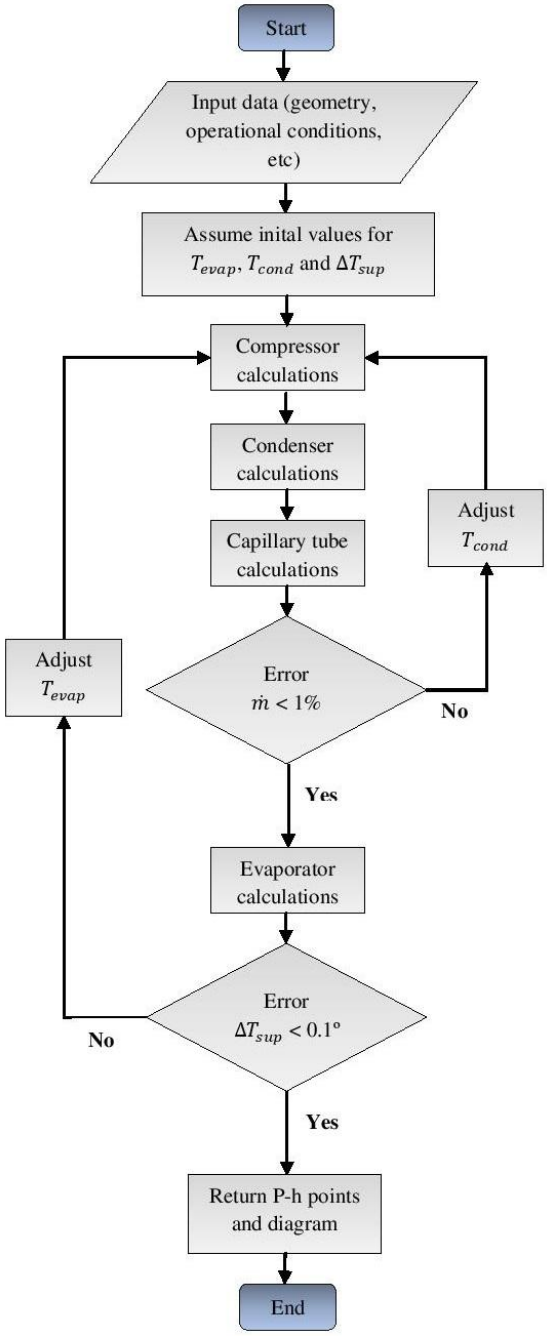

Figure 4 – Numerical scheme for system-level calculations

5. MODEL VALIDATION

The sub models of each component were validated individually with experimental data obtained from literature. The compressor chosen for model validation is the 1/5 HP VEMX5C manufactured by Embraco. Experimental data was obtained from a data sheet provided by the manufacturer. The non-linear curve fitting for semi empirical parameters that define the volumetric and overall efficiencies resulted in $C=0.03371$, $\delta P=0.2344$, $\alpha=0.7595$ and β=-10.31. The comparison between experimental data and model estimations for mass flow rate and required power are shown in Fig. 5-a and 5-b.

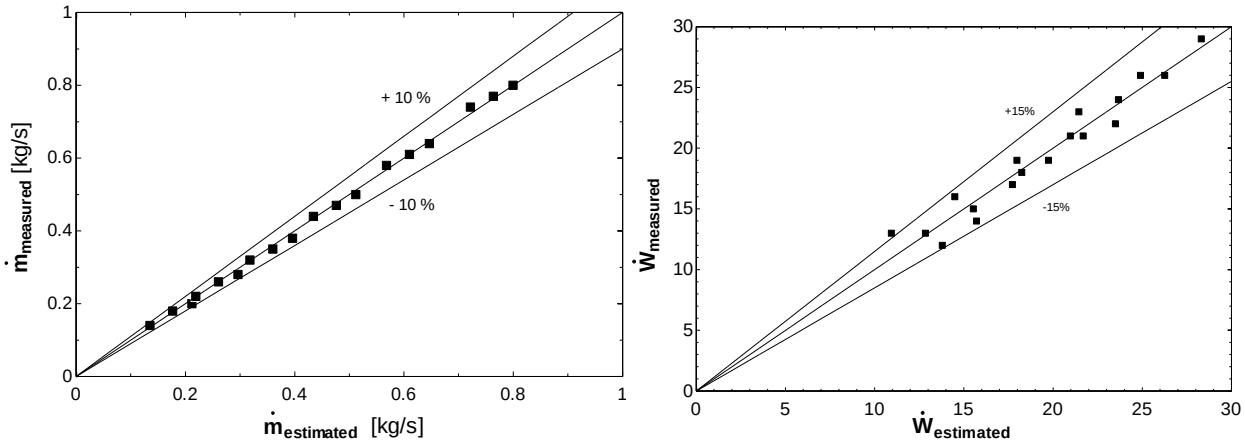

Figure 5-a (left) and 5-b (right). Validation results for the volumetric and overall efficiency semi-empirical models.

The adiabatic capillary submodel was validated for the refrigerant HC-600a using 35 experimental data points obtained from Schenk and Oellrich (2013) and Melo et al. (1999), as shown in Fig. 6, covering internal diameters from 0.611 to 0.77 mm and tube lengths from 2.01 to 3.93 m.

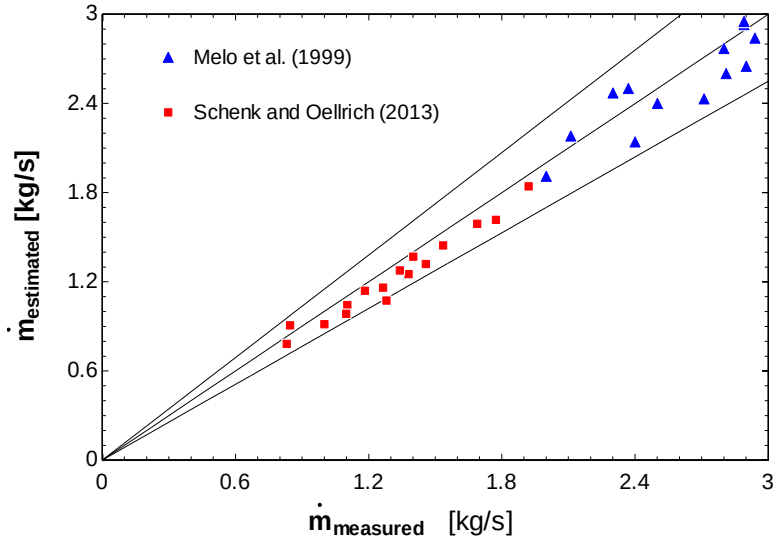

Figure 6 – Comparison between experimental data from Melo et. Al. (1999) and Schenk and Oellrich (2013) with Hermes, Melo and Knabben (2010) adiabatic capillary tube model.

The roll-bond evaporator submodel was validated using experimental data gathered from a research report by Melo, Silva and Silveira (1998), in which five different conditions were tested for a fixed evaporator geometry, whose characteristics are given in Tabs. 1 and 2. For the validation of the wire-and-tube condenser sub model, experimental data was obtained from Hermes (2000) for a single geometry detailed in Tab. 3. The validation results are shown in Tab. 4 that presents a comparison between the model and the experimental results for three operational conditions.

Table 1. Roll-bond evaporator geometrical dimensions (Rectangular Plate).

Dimension	Value
Height	480 mm
Width	300 mm
Plate Thickness	1.5 mm
Refrigerant Circuit Length	4568 mm
Refrigerant Circuit Diameter	10 mm

Table 2. Roll-bond evaporator sub model validation with experimental data from Melo, Silva and Silveira (1998).

Inlet Pressure [kPa]	Inlet Enthalpy [kJ/kg]	Mass flow rate [kg/h]	Temp. of Refrigerated Compartment [°C]	Avg. Temp. of Evaporator Surface [°C]	Measured Heat Transfer Rate [W]	Calculated Heat Transfer Rate [W]	Error [%]
121	88.6	2.91	-3.2	-19.5	43.7	37.9	-13.2
123	88.6	1.38	-4.7	-20.2	37.6	34.7	-7.8
124	88.6	2.38	-3.9	-19.9	39.8	36.1	-9.2
122	88.0	1.53	-4.0	-19.8	39.9	36.1	-9.6
120	88.4	0.93	-5.4	-20.3	37.0	33.6	-9.3

Table 3. Wire-and-tube condenser geometrical dimensions (Rectangular grid).

Dimension	Value
Height	840 mm
Width	470 mm
Tube Internal Diameter	3.34 mm
Tube External Diameter	4.76 mm
Tube Pitch	56 mm
Wire Diameter	1.5 mm
Wire Pitch	4.52 mm
No. of Tube Passes	15
No. of Wire Pairs	104

Table 4. Wire-and-tube condenser sub model validation with experimental data from Hermes (2000).

Inlet Pressure [kPa]	Inlet Temperature [°C]	Mass flux [kg/m^2.s]	Ambient Temperature [°C]	Measured Heat Transfer Rate [W]	Calculated Heat Transfer Rate [W]	Error [%]
1180	74.9	46.3	32	79	83.26	5.39
1553	89.7	56.4	43	88.8	96.7	8.9
2005	102.6	70.1	54	98.3	114.8	16.79

6. RESULTS AND DISCUSSIONS

After validating each component individually, a few system-level simulations were performed in order to compare the performance differences between a refrigeration cycle operating with HC-600a and HFC-134a, fixing the same geometries for the evaporator and condenser. The compressor model used for HFC-134a is the VEMY3H and VEMZ5C for HC-600a, both manufactured by Embraco and with a nominal power rating of 1/10 HP. The ambient temperature was estimated for two different conditions in order to assess the performance in a warmer day (27 °C) and a colder day (15 °C). Its assumed a fixed saturation temperature for the evaporator of -20 °C and 0 °C for the refrigerated compartment for all simulations. The P-h diagram of the results is found in Fig. 7 and the performance parameters in Tab. 5.

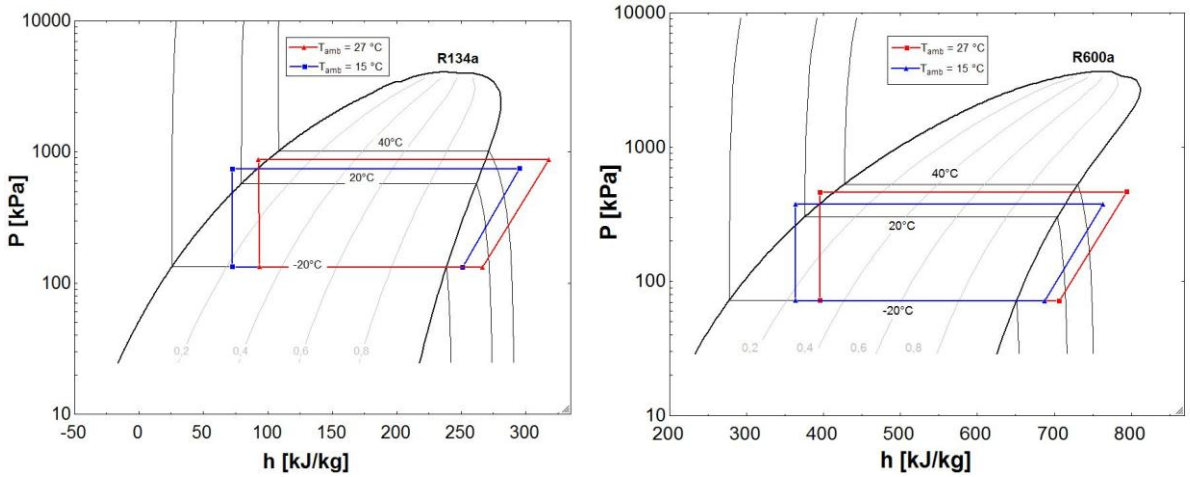

Figure 7 – Calculated P-h diagrams for HFC-134a (left) and HC-600a (right)

Table 5. Comparison between the system-level performance for a system operating with HFC-134a and the other with HC-600a maintaining a fixed evaporator and condenser geometry.

	HFC-134a		**HC-600a**	
T evaporator [°C]	-20	-20	-20	-20
T ambient [°C]	15	27	15	27
T compartment [°C]	0	0	0	0
Mass flow rate [kg/hr]	1.413	1.243	0.744	0.701
Tsat condenser [°C]	28.87	34.38	27.49	35.01
ΔP condenser [kPa]	2.4	3.0	3.5	3.9
ΔP evaporator [kPa]	0.9	0.6	0.96	0.82
Q evaporator [W]	71.03	61.20	68.16	62.12
Q condenser [W]	86.26	79.17	81.08	75.63
Compressor Combined Eff. (%)	56.57	63.74	57.06	54.43
W compressor [W]	15.23	17.97	12.92	13.51
COP	2.64	2.17	3.01	2.50
COP/COP Carnot (%)	14.50	21.45	16.53	24.71

From Tab. 5 its clear that the system with HC-600a operates more efficiently than the system with HFC-134a, even tough the pressure drop in the heat exchangers is higher in the former, which is partially explained by the higher specific volume of HC-600a since the geometry is fixed. The cooling load varies only marginally between the two refrigerants when the ambient temperature is fixed. The mass flow rate reduces with an increase on the ambient temperature, which is in agreement with experimental trends observed in reality.

7. CONCLUSION

In conclusion, a simplified methodology for predicting the steady-state thermal-hydraulic behavior of a small capacity vapor compression refrigeration system operating under HC-600a and HFC-134a was proposed and the components were validated individually against data gathered in literature. The model predictions for individual component showed, in general, a satisfactory agreement within ±15% error band. A system-level calculation was performed with success for both refrigerants, achieving convergence criteria for a couple of operational conditions. The HC-600a refrigerant showed a superior efficiency when compared to HFC-134a for all the conditions simulated.

8. ACKNOWLEDGEMENTS

The authors gratefully acknowledge the financial support given by CAPES (Coordination for the Improvement of Higher Level Personal, Brazil) and CNPq (National Council of Technological and Scientific Development, Brazil).

9. REFERENCES

Bansal, P.K. and Chin, T.C., 2003. Modelling and Optimisation of Wire-and-Tube Condenser. International Journal of Refrigeration, Vol. 26, No. 5, pp. 601-613.

Borges, B.N., Melo, C. and Hermes, C.J.L., 2015. Transient simulation of a two-door frost-free refrigerator subjected to periodic door opening and evaporator frosting. Applied Energy, Vol. 147, pp. 386-395.

Hermes, C.J.L., Melo, C. and Knabben, F.T., 2010. Algebraic solution of capillary tube flows. Part I: Adiabatic Capillary Tubes. Applied Thermal Engineering, Vol. 30, No. 5, pp. 449-457.

Churchill, S.W, 1977. Friction-factor equation spans all fluid-flow regimes. Chemical engineering, Vol. 84, No. 24, pp. 91-92.

Churchill, S.W. and Chu, H.H., 1975. Correlating equations for laminar and turbulent free convection from a vertical plate. International journal of heat and mass transfer, Vol. 18, No. 1, pp. 1323-1329.

Colebrook, C.F., 1939. Turbulent flow in pipes, with particular reference to transition region between the smooth and rough pipe laws. Journal of the Institution of Civil engineers, Vol. 12, No. 8, pp. 393-422.

Didi, M.B.O., Kattan, N. and Thome, J.R., 2002. Prediction of two-phase pressure gradients of refrigerants in horizontal tubes. International Journal of refrigeration, Vol. 25, No. 7, pp. 935-947.

Domanski, P.A. and McLinden, M.O., 1992. A simplified cycle simulation model for the performance rating of refrigerants and refrigerant mixtures. International journal of refrigeration, Vol. 15, No. 2, pp. 81-88.

Gnielinski, V., 1976. New equations for heat and mass-transfer in turbulent pipe and channel flow. International chemical engineering, Vol. 16, No. 2, pp. 359-368.

Gossard, J.J., Han, X., Ramalingam, M. and Sommers, A.D., 2013. Investigating the thermal-hydraulic performance of new refrigerant mixtures through numerical simulation of minichannel and microchannel evaporators. Applied Thermal Engineering, Vol. 50, No. 1, pp. 1291-1298.

Grönnerud, R., 1972. Investigation of liquid hold-up, flow-resistance and heat transfer in circulation type evaporators, part IV: two-phase flow resistance in boiling refrigerants. Bull. De l'Inst. Du Froid, Annexe, Vol. 1.

Hermes, C.J.L and Melo, C., 2008. A first-principles simulation model for the start-up and cycling transients of household refrigerators. International Journal of refrigeration, Vol. 31, No. 8, pp. 1341-1357.

Hermes, C.J.L and Melo, C., 2009. Assessment of the energy performance of household refrigerators via dynamic simulation. Applied Thermal Engineering, Vol. 29, No. 5, pp. 1153-1165.

Hermes, C.J.L., 2000. Desenvolvimento de modelos matemáticos para a simulação numérica de refrigeradores domésticos em regime transiente. Master's Thesis, Universidade Federal de Santa Catarina, Florianópolis, SC, Brazil.

Jahnig, D.I., Reindl, D.T. and Klein, S.A., 2000. A semi-empirical method for representing domestic refrigerator/freezer compressor calorimeter test data. ASHRAE Transactions, Vol. 106, pp. 122.

Klein, S.A. and Reindl, D.T., 1999. ASHRAE RP-870.

Klein, S.A. and Alvarado, F.L., 2002. Engineering equation solver. F-Chart Software, Madison, WI, Vol. 1.

Koury, R.N.N., Machado, L. and Ismail, K.A.R., 2001. Numerical simulation of a variable speed refrigeration system. International journal of refrigeration, Vol. 24, No. 2, pp. 192-200.

Liu, Z. and Winterton, R.H.S., 1991. A general correlation for saturated and subcooled flow boiling in tubes and annuli, based on a nucleate pool boiling equation. International journal of heat and mass transfer, Vol. 34, No. 11, pp. 2759-2766.

Melo, C., Ferreira, R.T.S., Neto, C.B., Goncalves, J.M. and Mezavila, M.M., 1999. An experimental analysis of adiabatic capillary tubes. Applied thermal engineering, Vol. 19, No. 6, pp. 669- 684.

Melo, C., Silva, L.W. and Silveira, S.J., 1998. Evaporadores Roll-Bond. Research Report, Florianópolis: UFSC/EMBRACO, pp. 1.

Schenk, M. and Oellrich, L.R., 2014. Experimental investigation of the refrigerant flow of isobutane (R600a) through adiabatic capillary tubes. International Journal of Refrigeration, Vol. 38, pp. 275-280.

Shah, M.M., 1979. A general correlation for heat transfer during film condensation inside pipes. International Journal of heat and mass transfer, Vol. 22, No. 4, pp. 547-556.

Tagliafico, L. and Tanda, G., 1997. Radiation and natural convection heat transfer from wire-and-tube heat exchangers in refrigeration appliances. International Journal of Refrigeration, Vol. 20, No. 7, pp. 461-469.

Yilmaz, T. and Ünal, S., 1996. General equation for the design of capillary tubes. Journal of fluids engineering, Vol. 118, No. 1, pp. 150-154.

Zhang, C. and Ding, G., 2004. Approximate analytic solutions of adiabatic capillary tube. International Journal of Refrigeration, Vol. 27, No. 1, pp. 17-24.

10. RESPONSIBILITY NOTICE

The authors are the only responsible for the printed material included in this paper.